



# Experimental evidence that lignin-modifying enzymes are essential for degrading plant cell wall lignin by *Pleurotus ostreatus* using CRISPR/Cas9

Takehito Nakazawa  | Iori Yamaguchi | Yufan Zhang | Chinami Saka | Hongli Wu | Keita Kayama | Moriyuki Kawauchi | Masahiro Sakamoto | Yoichi Honda 

Graduate School of Agriculture, Kyoto University, Kyoto, Japan

## Correspondence

Yoichi Honda, Graduate School of Agriculture, Kyoto University, Oiwakecho, Kitashirakawa, Sakyo-ku, Kyoto 606-8502, Japan.  
Email: [honda.yoichi.5n@kyoto-u.ac.jp](mailto:honda.yoichi.5n@kyoto-u.ac.jp)

## Funding information

Grants-in-Aid for Scientific Research (KAKENHI), Grant/Award Numbers: 19H03017, 19F19095, 21K18224, 19K22332, 18KK0178, 18H02254; JSPS Bilateral Program (JPJSBP), Grant/Award Numbers: 120209920, 120208402

## Abstract

Lignin-modifying enzymes (LMEs), which include laccases (Lacs), manganese peroxidases (MnPs), versatile peroxidases (VPs), and lignin peroxidases (LiPs), have been considered key factors in lignin degradation by white-rot fungi because they oxidize lignin model compounds and depolymerize synthetic lignin *in vitro*. However, it remains unclear whether these enzymes are essential/important in the actual degradation of natural lignin in plant cell walls. To address this long-standing issue, we examined the lignin-degrading abilities of multiple *mnp/vp/lac* mutants of *Pleurotus ostreatus*. One *vp2/vp3/mnp3/mnp6* quadruple-gene mutant was generated from a monokaryotic wild-type strain PC9 using plasmid-based CRISPR/Cas9. Also, two *vp2/vp3/mnp2/mnp3/mnp6*, two *vp2/vp3/mnp3/mnp6/lac2* quintuple-gene mutants, and two *vp2/vp3/mnp2/mnp3/mnp6/lac2* sextuple-gene mutants were generated. The lignin-degrading abilities of the sextuple and *vp2/vp3/mnp2/mnp3/mnp6* quintuple-gene mutants on the Beech wood sawdust medium reduced drastically, but not so much for those of the *vp2/vp3/mnp3/mnp6/lac2* mutants and the quadruple mutant strain. The sextuple-gene mutants also barely degraded lignin in Japanese Cedar wood sawdust and milled rice straw. Thus, this study presented evidence that the LMEs, especially MnPs and VPs, play a crucial role in the degradation of natural lignin by *P. ostreatus* for the first time.

## INTRODUCTION

Lignocellulosic biomass has received extensive attention as a renewable organic resource as it offers an alternative to fossil resources. Each major component/polymer (cellulose, hemicellulose, and lignin) can be processed into various chemicals, including biofuels, bioplastics, and carbon fibre composites (Mainka et al., 2015; Ragauskas et al., 2014; Rosenboom et al., 2022). Extensive efforts have also been made to

produce biofuels economically (Keasling et al., 2021; Khan et al., 2018), which would be important in energy security and sustainable development. However, lignocellulose is complex: for example, lignin and hemicellulose are linked by covalent bonds (Nishimura et al., 2018; Watanabe & Koshijima, 1988). This facilitates efficient and eco-friendly isolation of each component to be used for difficult processing, especially polysaccharides (cellulose and hemicellulose) isolation by removing lignin from wood biomass. Biological pre-

treatment using microorganisms or enzymes is an eco-friendly method for delignification. However, unlike polysaccharides, the lignin-degrading abilities of most microbes are limited (Cragg et al., 2015).

White-rot fungi, which belong to the class *Agaricomycetes*, efficiently decompose lignin in wood biomass and other lignocellulosic components. Therefore, elucidating the underlying lignin-degrading mechanisms would contribute to developing efficient methods for lignin removal. Generally, it was thought that lignin degradation by white-rot fungi consists of the following three steps: depolymerization by extracellular enzymes, transportation of the degraded lignin fragments into hyphal cells, and metabolism/mineralization to produce adenosine triphosphate (del Cerro et al., 2021; Hatakka, 1994). The first step, depolymerization by white-rot fungi, is considered to be initiated by extracellular lignin-modifying enzymes (LMEs), including manganese peroxidases (MnPs; EC1.11.1.13), versatile peroxidases (VPs; EC1.11.1.16), lignin peroxidases (LiPs; EC1.11.1.14), and laccases (Lacs; EC1.10.3.2) based on the fact that they oxidize lignin model compounds and depolymerize synthetic lignin, including dehydrogenase polymer lignin, *in vitro* (Eggert et al., 1996; Higuchi, 2004; Kondo et al., 1990). However, these model compounds are low-molecular weight and water-soluble chemicals. Synthetic lignin has a relatively simple structure composed of a single building block. Natural lignin has water insoluble, more complex, recalcitrant, and composite structures connected or associated with other polymeric components in the plant cell wall. To date, no report indicates that LMEs are involved in natural lignin degradation by white-rot fungi. Thus, the actual mechanism for the biodegradation of natural lignin remains unclear using enzymological and biochemical analyses. Apart from this difficult situation, MnPs, VPs, and LiPs are still considered key players in lignin degradation because genes encoding these three kinds of enzymes are present in the genomes of white-rot fungi but not in other fungi with different ecological classifications, including brown-rot fungi that efficiently decompose cellulose but not lignin in lignocellulose (Arantes & Goodell, 2014; Floudas et al., 2012; Kersten & Cullen, 2014). Moreover, differential expression of LMEs (or LME-encoding genes) was repeatedly reported on wood sawdust media or solid wood substrates (Fernández-Fueyo, Castanera, et al., 2014; Miyauchi et al., 2017).

Analysing the lignin-degrading abilities of mutants that lack the function/activity of the LME(s) is an effective strategy for examining whether the enzymes are involved and play an important role in (or essential for) lignin degradation. Recently, molecular genetics studies on lignin degradation have been conducted in the white-rot fungus *Pleurotus ostreatus* in which reliable and efficient genetic transformation and the gene-targeting system were reported (Honda et al., 2000;

Matsunaga et al., 2017; Salame et al., 2012). As in almost all white-rot fungi, not single but multiple copies of LME-encoding genes are predicted in the genome of *P. ostreatus* PC9 (3 *vps*, 6 *mnp*s, and 10 *lacs*; Knop et al., 2015; Suetomi et al., 2015; Table 1). Some *P. ostreatus mnp/vp* were disrupted separately, and the phenotypes of the single-gene deletants were analysed. However, the ability of the *mnp3* or *vp1* deletants to decolor Orange II, a model compound, to examine Mn<sup>2+</sup>-dependent peroxidase in *P. ostreatus* (Salame et al., 2010) was slightly reduced (Salame et al., 2012, 2013). Furthermore, the *vp2* deletant exhibited a slightly reduced lignin-degrading ability compared with its parental strain, although *vp2* was predominantly expressed on the solid-state cotton stalk medium and Beech (*Fagus crenata*) wood sawdust media (BWS) at the transcription level (Nakazawa, Izuno, Horii, et al., 2017; Salame et al., 2014). These studies concluded that these LMEs are dispensable and not important, or some additional enzymes and/or mechanisms may play an important role(s) in lignin degradation by the fungus. Considering the broad range of substrates for LMEs and the involvement of the mediators for the radical oxidation (Ainarayana, 1995; Harvey et al., 1986; Kirk & Farrell, 1987; Marzullo et al., 1995; Pointing, 2001), it is plausible that each LME does not

TABLE 1 List of *Pleurotus ostreatus mnp*, *vp*, and *lac* genes.

Gene (previous designations) <sup>a,b</sup>	Protein ID <sup>c</sup>
<i>vp1 (mnp4)</i>	116738
<i>vp2 (mnp2)</i>	60432
<i>vp3 (mnp5)</i>	123383
<i>mnp1 (mnp1)</i>	115087
<i>mnp2 (mnp9)</i>	61491
<i>mnp3 (mnp3)</i>	51690
<i>mnp4 (mnp7)</i>	121638
<i>mnp5 (mnp6)</i>	52120
<i>mnp6 (mnp8)</i>	51713
<i>lac1</i>	90578
<i>lac2</i>	116143
<i>lac3</i>	123288
<i>lac4</i>	65894
<i>lac6</i>	81104
<i>lac7</i>	60400
<i>lac9</i>	81107
<i>lac10</i>	81117
<i>lac11</i>	90573
<i>lac12</i>	90834

<sup>a</sup>Current (previous) designations of the *Pleurotus ostreatus mnp/vp* genes as described by Knop et al. (2015).

<sup>b</sup>Pezzella et al. (2014) and Ursula Kües annotated *lac5* as a ferroxidase-encoding gene. The *lac8* gene is missing in the genome of PC9.

<sup>c</sup>The genome database of strain PC9 ([https://genome.jgi.doe.gov/PleosPC9\\_1/PleosPC9\\_1.home.html](https://genome.jgi.doe.gov/PleosPC9_1/PleosPC9_1.home.html)).

play a distinct role and that their function in lignin degradation is redundant. Nakazawa, Izuno, Kodera, et al. (2017), Nakazawa et al. (2019), Wu, Nakazawa, Morimoto, et al. (2021), Wu, Nakazawa, Xu, et al. (2021) identified transcriptional regulator-encoding genes in which single-gene mutations extremely reduced the lignin-degrading ability of *P. ostreatus* on BWS and milled rice straw medium (RS). Mn<sup>2+</sup>-dependent peroxidase (MnP) activities and *mnp/vp* transcript accumulation were reduced greatly in these strains (Wu et al., 2020). However, it remains unclear whether the inactivation of MnPs and VPs (*mnp*s and *vps*) causes the defects in wood lignin degradation by these mutant strains.

Therefore, it is necessary to generate and analyse multiple *mnp/vp/lac* deletants to address the long-standing issue: Are they important/essential in the degradation of lignin in natural lignocellulose by *P. ostreatus*? An efficient plasmid-based CRISPR/Cas9 was recently established in the fungus (Boontawon, Nakazawa, Horii, et al., 2021; Boontawon, Nakazawa, Inoue, et al., 2021). Using this technique, multiple-gene mutants can be obtained in one transformation experiment by expressing different sgRNAs concomitantly (Xu et al., 2022). In this study, we generated multiple-gene mutants of *mnp/vp/lac* and examined/compared

their wood lignin-degrading abilities to examine whether the LMEs play a dispensable role in wood lignin degradation by *P. ostreatus*.

## EXPERIMENTAL PROCEDURES

### Strains, culture conditions, and genetic techniques of *P. ostreatus*

The *P. ostreatus* strains used in this study are listed in Table 2. Yeast and malt extracts with glucose (YMG) medium (Rao & Niederpruem, 1969) solidified with 2% (wt/vol) agar in 9-cm and 4-cm Petri dishes were used for routine cultures. The cultures were maintained at 28°C under continuous darkness unless stated otherwise. The *P. ostreatus* strain PC9 (Table 2) was transformed using protoplasts prepared from mycelial cells as described by Salame et al. (2012). In this study, we excluded heparin and single-stranded lambda DNA.

To prepare the extracted substrate for BWS, a mixture of sawdust (100 g) and wheat bran (6 g) was first extracted using toluene and ethanol (450 mL; 2:1 vol/vol) for 1 h at 80°C four times. Then, 6 mL of tap water was added to a 6-cm glass plate containing the 2 g of extracted substrate to prepare BWS-I. Wheat bran was

TABLE 2 The *Pleurotus ostreatus* strains used in this study.

Strain	Genotype/description <sup>a,b</sup>	Source
PC9	A2B1	Larraya et al. (1999)
20b	A2B1 <i>ku80::Cbx<sup>R</sup></i>	Salame et al. (2012)
$\Delta vp2^c$	A2B1 <i>ku80::Cbx<sup>R</sup> vp2::hph</i>	Salame et al. (2012)
<i>vp2vp3d#1</i>	A2B1 <i>ku80::Cbx<sup>R</sup> vp2::hph vp3::bar</i>	This study
<i>vp2vp3mnp3mnp6m#1</i>	A2B1 <i>hyg<sup>R</sup>/a</i> quadruple mutant of the indicated genes derived from PC9	This study
<i>vp2vp3mnp3mnp6m2#1</i>	A2B1 <i>hyg<sup>R</sup> BF<sup>R</sup>/a</i> quadruple mutant of the indicated genes derived from <i>vp2vp3mnp3mnp6m#1</i> <sup>d</sup>	This study
<i>vp2vp3mnp3mnp6m2#2</i>	A2B1 <i>hyg<sup>R</sup> BF<sup>R</sup>/a</i> quadruple mutant of the indicated genes derived from <i>vp2vp3mnp3mnp6m#1</i> <sup>d</sup>	This study
<i>vp2vp3mnp2mnp3mnp6m#1</i>	A2B1 <i>hyg<sup>R</sup> BF<sup>R</sup>/a</i> quintuple mutant of the indicated genes derived from <i>vp2vp3mnp3mnp6m#1</i>	This study
<i>vp2vp3mnp2mnp3mnp6m#2</i>	A2B1 <i>ku80::Cbx<sup>R</sup> rho1b::hph/a rho1b</i> disruptant derived from 20b	This study
<i>vp2vp3mnp3mnp6lac2m#1</i>	A2B1 <i>hyg<sup>R</sup> BF<sup>R</sup>/a</i> quintuple mutant of the indicated genes derived from <i>vp2vp3mnp3mnp6m#1</i>	This study
<i>vp2vp3mnp3mnp6lac2m#2</i>	A2B1 <i>hyg<sup>R</sup> BF<sup>R</sup>/a</i> quintuple mutant of the indicated genes derived from <i>vp2vp3mnp3mnp6m#1</i>	This study
<i>vp2vp3mnp2mnp3mnp6lac2m#1</i>	A2B1 <i>hyg<sup>R</sup> BF<sup>R</sup>/a</i> sextuple mutant of the indicated genes derived from <i>vp2vp3mnp3mnp6m#1</i>	This study
<i>vp2vp3mnp2mnp3mnp6lac2m#2</i>	A2B1 <i>hyg<sup>R</sup> BF<sup>R</sup>/a</i> sextuple mutant of the indicated genes derived from <i>vp2vp3mnp3mnp6m#1</i>	This study

<sup>a</sup>*Cbx<sup>R</sup>* and *bar* indicate the carboxin and bialaphos resistance gene, respectively (Honda et al., 2000; Matsunaga et al., 2017).

<sup>b</sup>*hyg<sup>R</sup>* and *BF<sup>R</sup>* indicate resistance to hygromycin and bialaphos conferred by introducing CRISPR/Cas9 plasmids, respectively.

<sup>c</sup>Formerly, it was designated as  $\Delta mnp2$  because *vp2* was previously called *mnp2*.

<sup>d</sup>Neither *mnp2* nor *lac2* mutation was introduced by the bialaphos resistance transformation.

mixed with BWS to enhance ligninolytic enzyme production (Pickard et al., 1999; Tsukihara et al., 2006). BWS-II (1.9 g of unextracted substrate, 0.1 g of unextracted wheat bran, and 6 mL of tap water) and BWS-III (4.1 g of unextracted substrate, 0.3 g of unextracted wheat bran, and 10.6 mL of tap water) were also used in this study.

To prepare the extracted substrates for Cedar (*Cryptomeria japonica*) wood sawdust media (CWS) and RS, Cedar sawdust (50 g), rice straw (50 g), and wheat bran (50 g) were separately extracted using toluene and ethanol (2:1 vol/vol; 300 mL) for 1 h at 80°C five, four, and five times, respectively. The CWS and RS composition are as follows: 1.9 g of extracted Japanese cedar sawdust, 0.1 g of extracted wheat bran, 6 mL of tap water; 0.95 g of extracted rice straw, 0.05 g of extracted wheat bran, and 3 mL of tap water (in each 6-cm glass plate).

Beech wood sawdust, Japanese cedar sawdust, rice straw, and wheat bran used in this study were purchased from Shinkoen (Gifu, Japan), Shinkoen, Honda nojo (Ishikawa, Japan), and Nisshin Seifun (Tokyo, Japan), respectively. They included moisture because they were stored at 4°C or room temperature. The sawdust and rice straw used to prepare BWS-II, BWS-III, CWS, and RS were subject to size-fractionation (250–500 µm), whereas that used to prepare BWS-I was not (almost all the particles were smaller than 2 mm). These solid cultures were stationarily maintained at 28°C under continuous darkness.

## RNA-seq and quantitative reverse transcription-polymerase chain reaction

Each *P. ostreatus* strain was grown on BWS-I, followed by total RNA extraction using the FastGene RNA Premium kit (NIPPON Genetics, Tokyo, Japan). RNA-seq and bioinformatics analysis were performed as described by Wu, Nakazawa, Morimoto, et al. (2021) and Wu, Nakazawa, Xu, et al. (2021), except that transcripts per million (TPM) values were calculated/used to compare transcriptional expression levels.

Reverse transcription and quantitative polymerase chain reaction (PCR) using real-time PCR were performed as described by Nakazawa et al. (2019) and Pfaffl (2001). RNA-seq data and primer pairs used to amplify cDNA fragments and their amplification efficiencies are given in Tables S2 and S3, respectively.

To perform quantitative reverse transcription-PCR (qRT-PCR) using the droplet digital PCR system QX200 (Biorad, California), each sample (1 ng [or 4 ng] of total RNA from 20b grown on BWS [CWS and RS] for 13 and 20 days) was reverse-transcribed using the PrimeScript RT kit (Takara, Shiga, Japan), followed by droplet generation, the PCR reaction, and droplet reading according to manufacture instructions. The ddPCR Supermix for Probe (no dUTP; Biorad, California)

served as the PCR master mix. Primers and probes used for the digital PCR are given in Tables S3 and S4.

## Design of sgRNAs targeting each *mnp/vp*

The different sgRNA sequences used to target *vp3*, *mnp2*, *mnp3*, *mnp6*, and *lac2* were designed as described by Boontawon, Nakazawa, Horii, et al. (2021) and Boontawon, Nakazawa, Inoue, et al. (2021). The targeting *vp2* was designated by Xu et al. (2022).

## Plasmid construction

The plasmid for disrupting the *vp3* gene (Protein ID: 123383; Table 1) was constructed as previously described by Nakazawa and Honda (2015). Briefly, a genomic fragment (Scaffold\_2:3,245,049–3,248,856 in the genome database of *P. ostreatus* strain PC9), amplified by PCR using the primer pair TN193/TN196 (Table S1), was cloned into pBluescript II KS+ digested with *EcoRV*. Inverse PCR was performed using the resulting plasmid as a template with the primer pair TN194/TN195. A DNA fragment containing the bialaphos-resistance gene, *bar*, was also amplified, with pZeroAct\_ppBRA (Matsunaga et al., 2017) serving as a template with the primer pair M13F/M13R. The resulting two DNA fragments were fused using the GeneArt Seamless Cloning and Assembly kit (Life Technologies, California) to yield a plasmid containing the *vp3*-disrupting cassette.

The four different plasmids used to introduce a single-gene mutation in *vp2*, *vp3*, *mnp3*, or *mnp6* were constructed as described by Boontawon, Nakazawa, Horii, et al. (2021) and Boontawon, Nakazawa, Inoue, et al. (2021). Briefly, the double-stranded DNA containing the sgRNA sequence targeting each *mnp/vp*, prepared by annealing two DNA oligonucleotides (primers YF37/YF38 [*vp2*], YF43/YF44 [*vp3*], YF29/YF30 [*mnp3*], and YF35/YF36 [*mnp6*]), was separately inserted into the *BsaI* site of the linearized.

pCcPef3-126 vector (Boontawon, Nakazawa, Horii, et al., 2021; Boontawon, Nakazawa, Inoue, et al., 2021; from Prof. Osakabe, Tokushima University) using the Golden Gate assembly (Engler et al., 2008). The target sites are 258–278(–), 487–506(+), 135–154(+), and 286–305(+) from their hypothesized start codons. The sgRNA insertion into the plasmids was verified using Sanger sequencing. The resulting plasmids were named pCcPef3-126-*vp2*, pCcPef3-126-*vp3*, pCcPef3-126-*mnp3*, and pCcPef3-126-*mnp6*, respectively. It was confirmed that a mutation in each *mnp/vp* was frequently (75%–100%) introduced into the hygromycin B-resistant strains transformed with each plasmid (Xu et al., 2022; data not shown).

To replace the *hph* (the hygromycin B resistance gene) cassette in pCcPef3-126 with the *bar* cassette



from pFNCB (Nguyen et al., 2020), inverse PCR was performed using pCcPef3-126 as a template with the primer pair TK9/TK10, followed by fusion with the fragment amplified from pFNCB with YN1/TK15 using the NEBuilder Hi-Fi DNA Assembly Cloning Kit (New England Biolabs, Massachusetts). The resulting plasmid was designated as pCcPef3-127. The two plasmids used to introduce a single-gene mutation in *mnp2* or *lac2* were constructed as described above using the Golden Gate assembly and DNA oligonucleotides YF91/YF92 (*mnp2*) and IY20/IY21 (*lac2*). The target sites are 1286–1306(–) and 170–189(–) from their start codons. The resulting plasmids were named pCcPef3-127-*mnp2* and pCcPef3-127-*lac2*, respectively.

To construct the pCcPef3-126-based plasmids containing two expression cassettes of two different sgRNAs, inverse PCR was conducted using pCcPef3-126-*mnp3* (A) and pCcPef3-126-*mnp6* (B) with IY2/IY3, separately. The sgRNA-expressing cassettes of *vp2* (C) and *vp3* (D) and the *P. ostreatus u6a* promoter (Xu et al., 2022; Scaffold\_9:233,432–233,925) (E) were also amplified from pCcPef3-126-*vp2*, pCcPef3-126-*vp3*, and the PC9 genome with IY6/IY5, IY7/IY5, and IY8/IY9, respectively. The three fragments, (A) (C) (E) or (B) (D) (E), were fused using the NEBuilder Hi-Fi DNA Assembly Cloning Kit (New England Biolabs, Massachusetts). The resulting plasmids were designated as pCcPef3-126-*mnp3vp2* and pCcPef3-126-*mnp6vp3*. Similarly, the expression cassette for sgRNA targeting *lac2* amplified from pCcPef3-127-*lac2* using IY29/IY5, the inverse PCR product from pCcPef3-127-*mnp2* (IY2/IY3), and (E) were fused to construct pCcPef3-127-based plasmids containing two expression cassettes of two different sgRNAs targeting *mnp2* and *lac2*, which was designated as pCcPef3-127-*mnp2lac2*.

## Genomic PCR

Rapid colony PCR was conducted to verify gene mutations as described by Boontawon, Nakazawa, Horii, et al. (2021) and Boontawon, Nakazawa, Inoue, et al. (2021). The EmeraldAmp PCR Master Mix (Takara, Shiga, Japan) and the KDO FX Neo (TOYOBO, Tokyo, Japan) were used in this study. The PCR conditions were as follows: 35 cycles at 95°C (30 s), 55°C (30 s), and 72°C (60 s) for the EmeraldAmp; one cycle at 95°C (2 min) for initial denaturation, 35 cycles at 98°C (15 s), 58°C (30 s), and 68°C (30 s).

## Southern blot analysis

Genomic DNA was extracted from each strain via the cetyl trimethyl ammonium bromide method as described by Muraguchi et al. (2003) and Zolan and Pukkila (1986). The extracted DNA (~3 µg) was subject

to Southern blot analysis as described by Nakazawa et al. (2023). Restriction enzymes to digest genomic DNA and primers to amplify a genomic fragment for a probe were *XhoI* and TN1022/TN1023 (*vp2*), *PstI* and TN1422/TN1423 (*vp3*), *HindIII* and *BamHI*, and TN1426/TN1427 (*mnp2*), *XhoI* and TN1430/TN1431 (*mnp3*), *XhoI* and TN1424/TN1425 (*mnp6*), *XhoI* and TN1428/TN1429 (*lac2*), respectively.

## Quantification of ergosterol

Each *P. ostreatus* strain was grown on BWS-I for 20 days, followed by freeze-drying. The total weight of each sample (freeze-dried BWS containing hyphal cells) was measured. Each sample (~0.5 g) was immediately maintained at 55°C for 24 h to dry out, and the weight was measured. Then, it was incubated in 7 mL 1N KOH (90:10[vol/vol], methanol: pure water) for 2 h at 80°C. The resulting sample (600 µL) was subject to extraction using an equal volume of hexane thrice. Cholesterol (Fujifilm, Tokyo, Japan) was added as the internal standard, followed by solvent removal using a rotary evaporator. The sample was dissolved in chloroform and acetonitrile (1:1, vol/vol). A reversed-phase high-performance liquid chromatography (HPLC) analysis was conducted using Aqua 5-µm C18 125A (4.6 mm i. d. × 250 mm; Phenomenex, Torrance, California). The solvents for isocratic elution were acetonitrile, hexane, and isopropanol (89:10:1, vol/vol). Ergosterol and cholesterol were monitored at 210 and 280 nm, respectively, using the photodiode array detector SPD-M20A (Shimadzu, Kyoto, Japan). The amount of ergosterol in each sample was calculated using the standard curve generated via quantitative analyses of the ergosterol standard (Fujifilm, Tokyo, Japan). Based on these data, the total ergosterol in each plate was calculated to estimate fungal biomass. In this study, the ergosterol content in fungal biomass (mycelial cells) of *P. ostreatus* (1.32% [wt/wt]) was determined, as shown in Figure S7.

## Assay for extracellular enzyme activity

Each *P. ostreatus* strain was grown on BWS-I for 13, 20, and 30 days, followed by the assay for extracellular Mn<sup>2+</sup>-dependent and H<sub>2</sub>O<sub>2</sub>-dependent phenol oxidase (MnP) activity using 2-methoxyphenol (Wako, Tokyo, Japan) as a substrate according to Kamitsuji et al. (2004) and Nakazawa, Izuno, Koder, et al. (2017). MnP activity was calculated by subtracting the activity determined in the presence of H<sub>2</sub>O<sub>2</sub> from that in the presence of MnSO<sub>4</sub> and H<sub>2</sub>O<sub>2</sub>.

The extracellular cellobiosidase activity was estimated using 4-nitrophenyl β-D-cellobioside (Tokyo Chemical Industry, Tokyo, Japan) in this study. In this experiment, 50 µL of supernatant containing extracellular enzymes (with or without boiling at 95°C for 15 min)

and 5  $\mu$ L of 10 mM of each substrate (50% [vol/vol] dimethyl sulfoxide, DMSO) were mixed and incubated at 37°C for 1 h, followed by adding 150  $\mu$ L of 1 M Na<sub>2</sub>CO<sub>3</sub>. Absorbance at 405 nm of each boiled sample was subtracted from the non-boiled sample to calculate and compare the 4-nitrophenol released from each substrate (molar absorptivity is 18,500). The absorbance was measured using Multiskan GO (Thermo Fisher, Massachusetts).

## Quantification of Klason lignin

Each *P. ostreatus* strain was grown on BWS-II (BWS-III) for 20 and 30 days (18 and 28 days), followed by solvent extraction using toluene and ethanol (2:1, vol/vol) as described by Nakazawa et al. (2019). The residual amount of Klason lignin (acid insoluble) contained in each BWS solution after cultivation of the *P. ostreatus* strains was quantified as previously described by Ritter et al. (1932). To compare the lignin degradation selectivity among the *P. ostreatus* mutants, changes in the lignin composition (percentage) of lignin contained in BWS-II were also calculated and compared.

Each strain was also grown on CWS and RS for 30 days to quantify the Klason lignin. In this case, solvent extraction after cultivation was conducted using acetone for 30 min twice at room temperature.

## RESULTS

### Identification of *mnp/vp/lac* genes highly expressed in *P. ostreatus* 20b

We previously performed RNA-sequencing (RNA-seq) on *P. ostreatus* 20b grown on the beech wood sawdust

medium I (BWS-I) for 13 days to analyse its transcriptional expression pattern (Wu et al., 2020). In this study, RNA-seq was further conducted at 20-day and 28-day culture periods to analyse the time-course expression of each *mnp/vp/lac*. As shown in Figure 1, the sum of the TPM values of *vp2* and *vp3* accounted for 78%–81%, 70%–74%, and 50%–51% of the total TPM of the 19 *mnp/vp/lac* at the 13-day, 20-day, and 28-day culture periods, respectively. Those of *vp2*, *vp3*, and *mnp3* accounted for 85%–86%, 85%–89%, and 82%–83% at the 13-day, 20-day, and 28-day culture periods, respectively. This result suggests that VP2 and VP3 are major LMEs under this culture condition at the 13-day and 20-day periods, whereas VP2, VP3, and MnP3 are at the 28-day ones. MnP2, Mnp6, and Lac2 are also possibly expressed somewhat, whereas the others are hard.

### The lignin-degrading ability of a *P. ostreatus* *vp2/vp3* double-gene deletant was not reduced

Considering the time-course transcriptional expression level of *P. ostreatus* *mnp/vp/lac*, we first examined the possibility that *vp2/vp3* double-gene deletion causes defects in lignin degradation on BWS. Therefore, we transformed the  $\Delta$ *vp2* strain (Table 2; Salame et al., 2012) using a plasmid containing a *vp3*-disrupting construct and isolated bialaphos-resistant strains. Genomic PCR experiments showed that the *vp3* gene was replaced with the *bar* gene in one transformant (Figure 2A,B). Therefore, we concluded that this strain was *vp2/vp3* double-gene deletant designated as *vp2vp3d#1* (Table 2).

To examine whether *vp2/vp3* double-gene deletion reduces the lignin-degrading ability, 20b and *vp2vp3d#1* were grown on BWS-III, followed by quantifying/

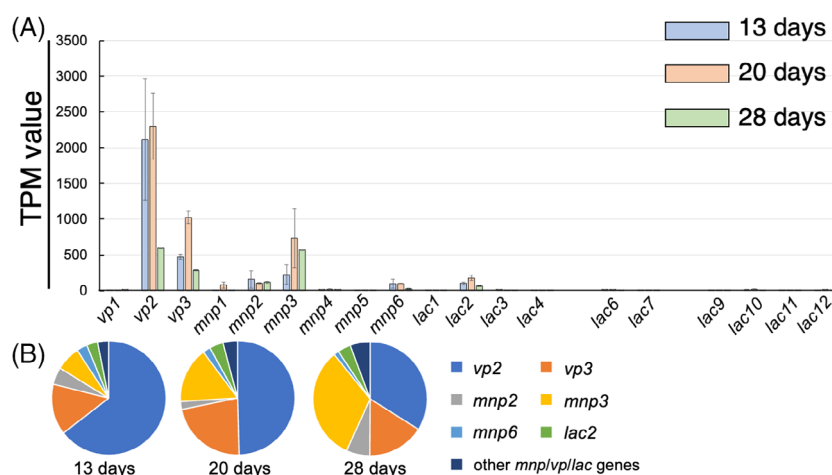


**FIGURE 1** Time-course transcriptional expression pattern of *mnp/vp/lac* genes in the *Pleurotus ostreatus* 20b strain on beech wood sawdust medium-I analysed using RNA-seq. (A) Transcripts per million (TPM) value of each gene at 13-day, 20-day, and 28-day culture periods. The graphs and bars represent the average and standard deviations, respectively ( $n = 2$ ). (B) Diagrams showing the percentage of TPM value of each gene at each culture period.

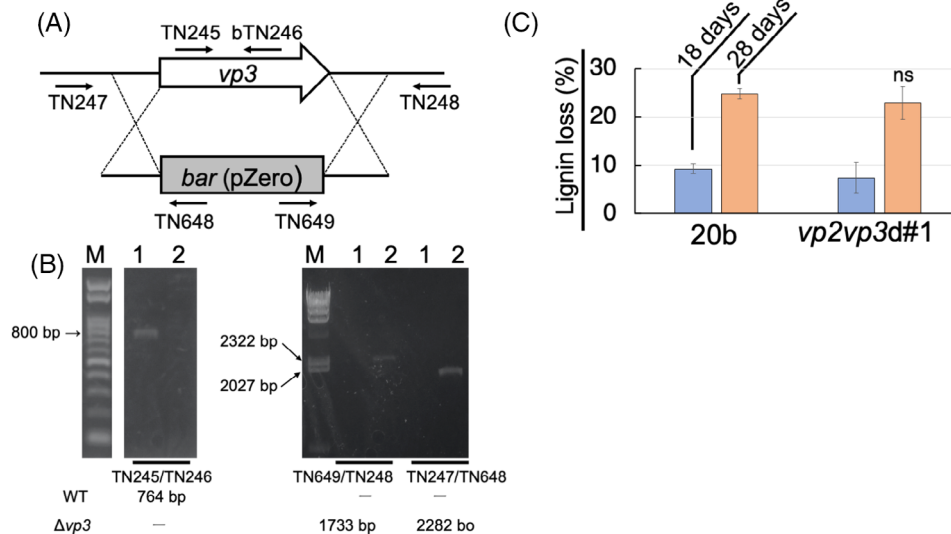


**FIGURE 2** Generation and analysis of the *vp2vp3* double-gene deletant (*vp2vp3d#1*) derived from the *vp2* single-gene deletant ( $\Delta vp2$ ) using homologous recombination. (A) A diagram of the genomic locus of *Pleurotus ostreatus* *vp3*. Black arrows indicate the primers used for the polymerase chain reaction (PCR) amplification. (B) Genomic PCR experiments confirming the *vp3* deletion in the double-gene deletants. Primers used in each PCR experiment are shown in (A). The expected size of each PCR-amplified genomic fragment was indicated. (C) The ability of the *vp2vp3d#1* strain to degrade lignin on beech wood sawdust medium (BWS)-III. The indicated strains, the double-gene deletant and its parental control 20b, were grown on BWS-III for 18 and 28 days. The decreased amount of Klason lignin was compared with that in the No-fungus control plate (onto which *P. ostreatus* had not been inoculated). The graphs and bars represent average and standard deviations, respectively ( $n = 2$  for 18-day samples;  $n = 3$  for 28 days ones). 'ns' indicates statistical non-significance ( $p > 0.05$ ) when statistical significance tests were performed against the parental control (at 28-day period) using a two-tailed equal variance *t*-test.

comparing the amount of Klason lignin. As shown in Figure 2C, the decreased amount of Klason lignin in the medium after growing the double-gene deletants was similar to that after growing its parental control, 20b ( $vp2^+vp3^+$ ). This result suggests that the lignin-degrading ability of *P. ostreatus* on BWS is not reduced by the *vp2/vp3* double-gene deletion.

### Isolation and characterization of *vp2/vp3/mnp3/mnp6* quadruple-gene mutant

To examine whether additional multiple *mnp/vp* mutations cause defects in lignin degradation, CRISPR/Cas9 was used instead of homologous recombination due to the limited transformation markers available in *P. ostreatus*. Based on the transcriptional expression level of each *mnp/vp/lac* (Figure 1), we selected *mnp3* and *mnp6*, combined with *vp2* and *vp3*, as targets. To generate the quadruple-gene mutants, plasmids pCcPef3-126-*mnp3vp2* and pCcPef3-126-*mnp6vp3* (see Experimental procedures section) were co-introduced into PC9 (Table 2), which resulted in 33 hygromycin-B-resistant transformants.

Next, we examined whether a mutation was introduced into each of the four genes (*vp2*, *vp3*, *mnp3*, or *mnp6*) in each transformant using genomic PCR experiments. Our previous studies showed that the introduced plasmid(s) were often integrated at the target site of sgRNA in some of the *P. ostreatus* mutants obtained

from the pCcPef3-126-based CRISPR/Cas9 (Boontawon, Nakazawa, Horii, et al., 2021; Boontawon, Nakazawa, Inoue, et al., 2021; Koshi et al., 2022; Yamasaki et al., 2022). This usually caused insufficient amplification from the mutants with large insertions due to the requirement of a longer extension time than the fragment amplified from the parental control strain. In this study, we aimed to screen such insertional mutants as the size of the PCR-amplified fragment can be easily distinguished between mutants and the parental control using conventional genomic PCR experiments. Therefore, primer pairs IY14/IY15 (*vp2*), IY16/IY17 (*vp3*), IY10/IY11 (*mnp3*), and IY12/IY13 (*mnp6*) were used separately (Figure 3A). Genomic fragments of the partial open reading frames (ORFs) of *vp2* (172 bp), *vp3* (213 bp), *mnp3* (142 bp), and *mnp6* (171 bp) containing the target sequences of sgRNA are expected to be amplified from PC9 when using the respective primer pairs (Scaffold 8:637,034–637,205, 2:3,247,277–3,247,489, 3:1,767,759–1,767,900, and 3:2,545,517–2,545,687 in the Joint Genome Institute (JGI) genome database of *P. ostreatus* PC9, respectively; [http://genome.jgi.doe.gov/PleosPC9\\_1/PleosPC9\\_1.home.html](http://genome.jgi.doe.gov/PleosPC9_1/PleosPC9_1.home.html)). As shown in Figure 3A, all four expected fragments were amplified from the PC9 strain but not from one transformant (Lane 4 in Figure 3A), when the EmeraldAmp Max was used. These results suggest that this strain is a *vp2/vp3/mnp3/mnp6* quadruple mutant.

In Figure 3A, the band observed in Lane 4 (*vp2* IY14/IY15) was re-amplified using the KOD FX Neo.

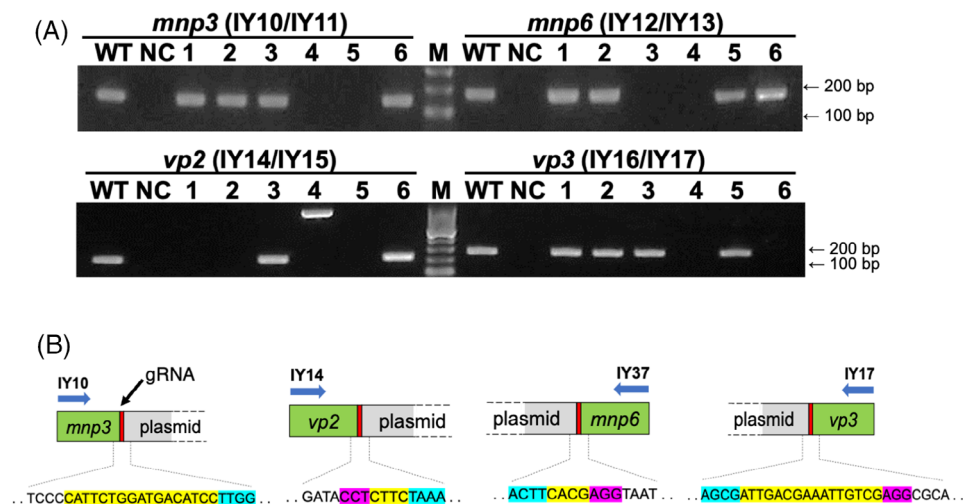


**FIGURE 3** Identification of the *vp2/vp3/mnp3/mnp6* quadruple-gene mutant. (A) Examples of genomic polymerase chain reaction (PCR) experiments using the EmeraldAmp to examine mutations in the indicated genes using the indicated primer pairs. Lane WT, the parental strain PC9 as a positive control; Lane NC, a negative control reaction into which genomic DNA was excluded; Lanes 1–6, obtained 6 out of a total of 33 transformants; Lane M, a 1 kb DNA ladder. (B) Identification of insertional mutations in *vp2*, *vp3*, *mnp3*, and *mnp6* of the quadruple mutants. For highlights in the nucleotide sequence: yellow shades indicate sgRNA, purple shades indicate PAM sequence and blue shades indicate plasmid sequence.

The about 3 kb fragment was also PCR-amplified from the possible quadruple-gene mutant when the KOD FX Neo (instead of the EmeraldAmp Max) was used with IY10/IY11 (data not shown). These PCR-amplified fragments were longer than that from PC9 (172 and 142 bp), suggesting that a portion of the plasmid sequences was integrated at the sites of the sgRNAs targeting *vp2* and *mnp3*. As shown in Figure 3B, this hypothesis was confirmed/proved via DNA sequencing of these two PCR-amplified fragments with IY14 and IY10, respectively. With the assumption that insertional mutations had also been introduced at the sgRNA target sites of *vp3* and *mnp6* of the possible quadruple mutant, we further performed genomic PCR to identify the *vp3* and *mnp6* mutations. The fragments were PCR-amplified with TN46/IY17 (*vp3*) and CI81/IY37 (*mnp6*). These fragments were subject to DNA sequencing with IY17 (*vp3*) and IY37 (*mnp6*), which revealed insertional mutations (Figure 3B).

In addition, we performed Southern blot analyses to ensure the quadruple gene mutation in the strain corresponding to Lane 4 of Figure 3A. As shown in Figure S1, the observed sizes of the detected band were different between this strain and its parental strain, PC9, when each probe for *vp2*, *vp3*, *mnp3*, or *mnp6* was hybridized with the genomic fragments digested with each restriction enzyme indicated in Figure S1. These results are not inconsistent with the idea that insertional mutations have been introduced. Altogether, we concluded that this strain (Lane 4 in Figure 3A) is a *vp2/vp3/mnp3/mnp6* quadruple-gene mutant; therefore, it was designated as *vp2vp3mnp3mnp6m#1* (Table 2).

To compare the hyphal growth rate between the *vp2vp3mnp3mnp6m#1* strain and the parental control PC9, they were grown on YMG agar plates for 9 days to measure the colony diameter of each strain. As shown in Figure 4A, a significance ( $p < 0.05$ ) was observed. However, the difference was minimal. Next, the amount of ergosterol contained in BWS-I, growing each strain for 20 days, was quantified to compare fungal biomass (Niemenmaa et al., 2008), reflecting the hyphal growth rate under this culture condition. As shown in Figure 4B, the amount per plate when the quadruple-gene mutant was cultured for 20 days was significantly (~31%) smaller than when PC9 was cultured. This result suggests that the mutant growth rate is lower than the parental control on BWS-I.

Next, to examine the effects of *vp2/vp3/mnp3/mnp6* quadruple-gene mutation on wood lignin degradation, PC9 and *vp2vp3mnp3mnp6m#1* were grown on BWS-I and BWS-II, followed by the comparison of extracellular enzyme activities and the decreased amount of Klason lignin. As shown in Figure 4C,D, Mn<sup>2+</sup>-dependent peroxidase (MnP) activity, which is mediated by both MnPs and VPs that oxidize Mn<sup>2+</sup> to Mn<sup>3+</sup> (Gold & Glenn, 1988; Knop et al., 2015; Ruiz-Dueñas et al., 1999; Salame et al., 2012), was almost lost in the quadruple mutant. In contrast, the extracellular cellobiosidase activity (hydrolyzation of 4-nitrophenyl β-D-cellobioside) was slightly higher in the mutant than in the parental control. Regarding lignin degradation in BWS-II, ‘Lignin loss’ (Figure 5A) was slightly lower in *vp2vp3mnp3mnp6m#1* than in PC9, with significance at both the 20-day and 30-day periods. This result suggests that the quadruple-gene mutant degrades lignin in



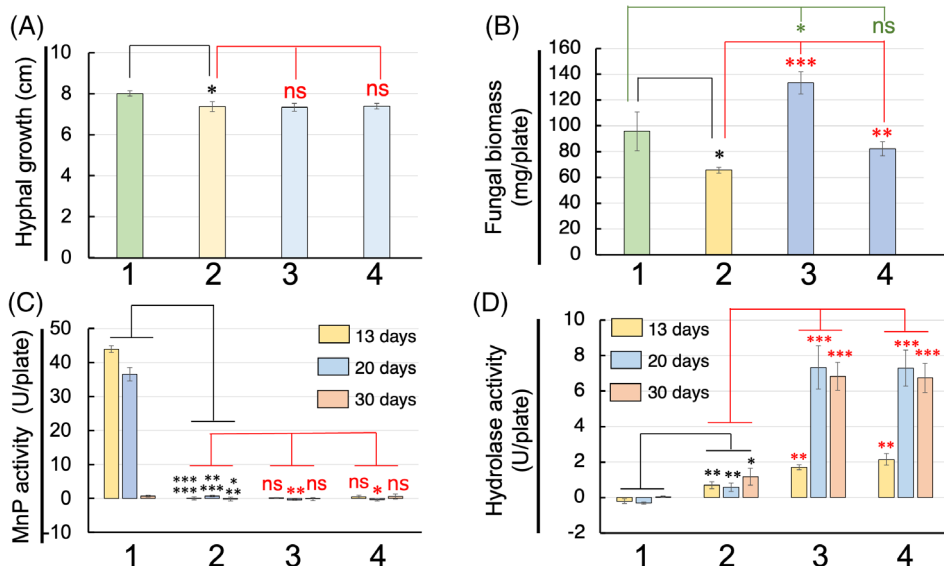


**FIGURE 4** Hyphal growth rates and extracellular enzyme activities of the *Pleurotus ostreatus* *vp2/vp3/mnp3/mnp6* quadruple-gene and *vp2/vp3/mnp2/mnp3/mnp6/lac2* sextuple-gene mutants on yeast and malt extracts with glucose (YMG) agar plate and beech wood sawdust medium (BWS)-I. (A) Hyphal growth rates of the indicated strains (1, the parental control PC9; 2, *vp2vp3mnp3mnp6m#1*; 3, *vp2vp3mnp2mnp3mnp6lac2m#1*; 4, *vp2vp3mnp2mnp3mnp6lac2m#2*) grown on YMG agar plate. Hyphal growth represents the diameter of colonies 9 days after inoculation. The graphs and bars represent the average and standard deviations, respectively ( $n = 3$ ). (B) Quantification of ergosterol in BWS-I growing each strain at 20-day culture period ( $n = 3$ ). ‘Fungal biomass’ indicates the amount (weight) of freeze-dried mycelial cells in each plate calculated based on the standard curve in Figure S7A. (C) MnP activity of the indicated strains grown on BWS-I for 13 and 20 days (substrate is 2-methoxyphenol). The graph and bars represent the average and standard deviations, respectively ( $n = 3$ ). One unit of activity for guaiacol oxidation was defined as the amount of enzyme that increased the absorbance at 465 nm by 1.0 per minute (D) Hydrolase activities of the indicated strains when 4-nitrophenyl  $\beta$ -D-cellobioside served as a substrate. The graph and bars represent the average and standard deviations, respectively ( $n = 3$ ). One unit was defined as the amount of enzyme that released 1- $\mu$ mol 4-nitrophenol per hour. Statistical significance tests between the parental PC9 and the quadruple-gene mutant (or between the quadruple-gene and the sextuple-gene mutants) were conducted using a two-tailed equal variance *t*-test. \* $p < 0.05$ , \*\* $p < 0.01$ , \*\*\* $p < 0.001$ , \*\*\*\* $p < 0.0001$ , \*\*\*\*\* $p < 0.00001$ , \*\*\*\*\* $p < 0.000001$ . ‘ns’ indicates statistical non-significance ( $p > 0.05$ ).

BWS-II lesser than in PC9. Furthermore, ‘Composition change’ (Figure 5B) was compared between the two strains. When this value (composition change) is negative, such as Lane 1 (PC9), lignin may be degraded more than polysaccharides (cellulose and hemicellulose). In a positive case, polysaccharides may be degraded more than lignin. Thus, the selectivity of lignin degradation may be estimated/compared, although apparent lignin content may be slightly affected by fungal biomass weight in BWS-II. Based on the results (Lanes 1 and 2 of Figure 5B), the amount of polysaccharide degraded by the quadruple-gene mutant may not be proportionally reduced to that of lignin.

### Isolation of quintuple and sextuple *mnp/lac* mutants

Quintuple-gene and sextuple-gene mutants were generated to examine the lignin-degrading abilities of further additional multiple-gene mutants. Based on the RNA-seq data, *mnp2* and *lac2* were selected as the genes to be mutated, with *vp2*, *vp3*, *mnp3*, and *mnp6*. Plasmid pCcPef3-127-*mnp2*, pCcPef3-127-*lac2*, or pCcPef3-127-*mnp2lac2* were separately introduced

into the *vp2vp3mnp3mnp6m#1* strain, and bialaphos-resistance transformants were obtained. As in the case of screening for the quadruple-gene mutant, genomic PCR was conducted using YF135/YF136 (*mnp2*; 872 bp) and IY24/IY25 (*lac2*; 494 bp; Scaffold 9:33,523–34,394 and 5:1,079,197–1,079,690, respectively). NO88/NO99, which amplifies a 752-bp genomic fragment from the ORF of the gene corresponding to Protein ID 64849 in the JGI genome database, also served as a positive control. When pCcPef3-127-*mnp2* or pCcPef3-127-*lac2* was introduced, a single-gene mutation in *mnp2* or *lac2* was suggested to be introduced into eight (Lanes 1, 2, 3, 5, 6, 7, 8, and 9 in Figure S2) and two (Lanes 2 and 10 in Figure S3) out of the obtained nine and eight transformants, respectively. Double-gene mutations in *mnp2* and *lac2* were also suggested to be introduced into 6 (Lanes 3, 9, 12, 13, 15, and 17 in Figure S4) out of the obtained 18 strains transformed with pCcPef3-127-*mnp2lac2*. Southern blot analyses also supported *mnp2* and *lac2* mutations in the two possible sextuple gene mutations (Figure S5). Based on these results, six strains used to examine the lignin-degrading abilities (two *vp2/vp3/mnp2/mnp3/mnp6*, two *vp2/vp3/mnp3/mnp6/lac2*, and two *vp2/vp3/mnp2/mnp3/mnp6/lac2* mutants indicated

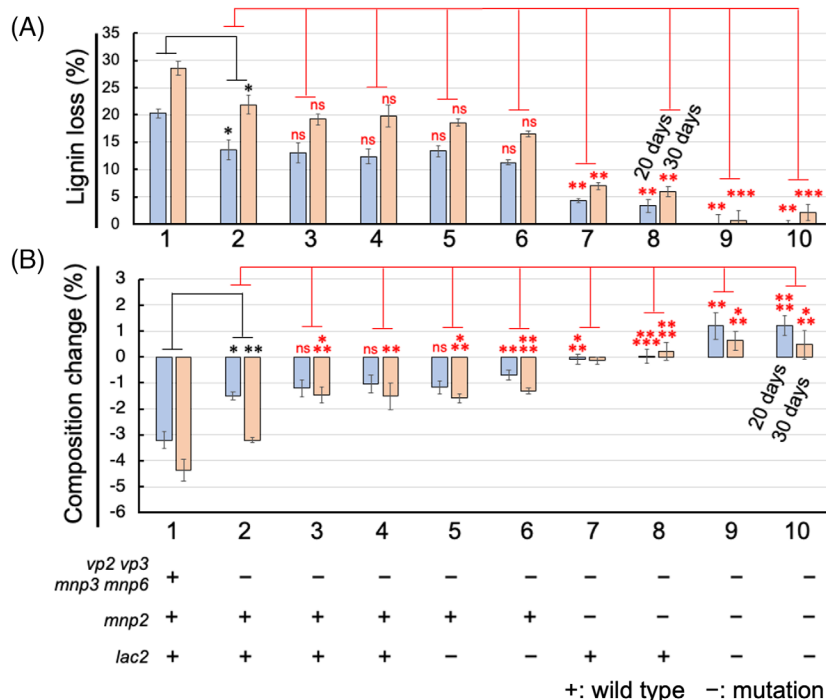


**FIGURE 5** The effects of the multiple-gene mutations on lignin degradation in beech wood sawdust medium (BWS)-II. (A) Comparison of the lignin-degrading abilities. ‘Lignin loss’ indicates the decreased amount of Klason lignin after growing each strain. The amount of Klason lignin contained in BWS-II on which the *Pleurotus ostreatus* strain was not inoculated was 0.402 g. (B) Comparison of the selectivity of lignin degradation. ‘Composition change’ indicates changes in the composition (percentage) of lignin contained in BWS-II after the fungal cultivation. The Klason lignin composition in BWS-II on which the *P. ostreatus* strain was not inoculated was 23.1% (wt/wt). The indicated strains (1–10) were grown on BWS-II for 20 and 30 days. The graphs and bars represent the average and standard deviations, respectively ( $n = 3$ ). Lane 1, the parental control PC9; 2, *vp2vp3mnp3mnp6m#1*; 3, *vp2vp3mnp3mnp6m2#1*; 4, *vp2vp3mnp3mnp6m2#2*; 5, *vp2vp3mnp3mnp6lac2m#1*; 6, *vp2vp3mnp3mnp6lac2m#2*; 7, *vp2vp3mnp2mnp3mnp6m#1*; 8, *vp2vp3mnp2mnp3mnp6m#1*; 9, *vp2vp3mnp2mnp3mnp6lac2m#1*; 10, *vp2vp3mnp2mnp3mnp6lac2m#2*. Statistical significance tests between the two indicated strains were performed using a two-tailed equal variance *t*-test. \* $p < 0.05$ , \*\* $p < 0.01$ , \*\*\* $p < 0.001$ , \*\*\*\* $p < 0.0001$ , \*\*\*\*\* $p < 0.00001$ , and \*\*\*\*\* $p < 0.000001$ . ‘ns’ indicates statistical non-significance ( $p > 0.05$ ).

in Figures S2–S4 and Table 2) were selected. Furthermore, two strains in which neither *mnp2* nor *lac2* was mutated (Lanes 7 and 10 in Figure S4), which were designated as *vp2vp3mnp3mnp6m2#1* (Lane 7) and *vp2vp3mnp3mnp6m2#2* (Lane 10) were selected (Table 2). To further confirm that neither *mnp2* nor *lac2* was mutated in these two strains, DNA sequencing was performed on the PCR-amplified genomic fragments (Figure S4) with YF135 or YF136 (*mnp2*) and IY24 or IY25 (*lac2*) as the primers. No mutations were observed within the fragments, suggesting that neither *mnp2* nor *lac2* was mutated in *vp2vp3mnp3mnp6m2#1* and *vp2vp3mnp3mnp6m2#2*.

### Lignin-degrading abilities reduced drastically in the *vp2/vp3/mnp2/mnp3/mnp6* and *vp2/vp3/mnp2/mnp3/mnp6/lac2* mutants on BWS

To examine the hyphal growth rate of the obtained two *vp2/vp3/mnp2/mnp3/mnp6/lac2* sextuple-gene mutants, they were grown on YMG agar plates for 9 days. As Figure 4A shows the diameter of the two strains was

similar to that of the parental control *vp2vp3mnp3mnp6m#1*. Regarding the amount of ergosterol per plate growing the sextuple-gene mutants, it was significantly larger than the parental quadruple-gene mutant (Figure 4B). Additionally, significantly higher extracellular cellobiosidase activities were observed in the two sextuple-gene mutants at the 20-day and 30-day period (Figure 4C,D).

To examine whether the quintuple-gene and/or sextuple-gene mutations cause defects in lignin degradation, the decreased amount of Klason lignin in BWS-II after cultivating the obtained mutants for 20 and 30 days was analysed. In this experiment, two of each multiple-gene mutant were selected and used to eliminate possible artefacts from additional ectopic integration and/or off-target effects, which might affect the degrading ability. As shown in Figure 5A, ‘lignin loss’ at both culture periods was significantly the same among the *vp2vp3mnp3mnp6m2#1* and #2 strains (Lanes 3 and 4), the *vp2vp3mnp3mnp6lac2* mutants (Lanes 5 and 6), and their parental *vp2vp3mnp3mnp6m#1* (Lane 2). While ‘Lignin loss’ of the *vp2vp3mnp2mnp3mnp6m#1* and #2 (Lanes 7 and 8) were lesser (about 1/3) than that of the *vp2vp3mnp3mnp6m#1*; ‘Lignin loss’ of the *vp2vp3mnp*

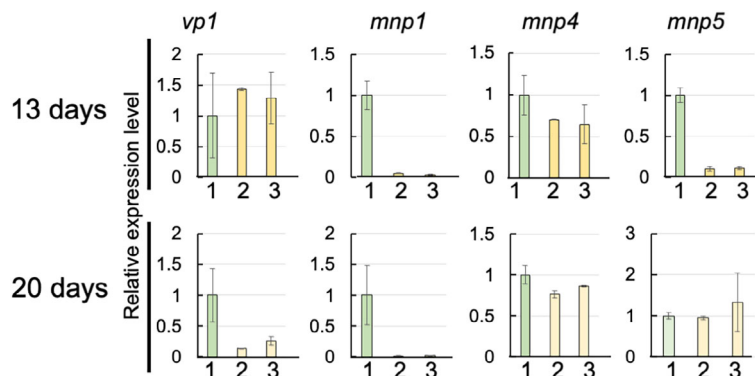


**FIGURE 6** Effects of the sextuple-gene mutations on transcript accumulation of *vp1*, *mnp1*, *mnp4*, and *mnp5* on beech wood sawdust medium-I at 13-day and 20-day culture periods using quantitative reverse transcription-polymerase chain reaction. The graphs and bars represent the average and standard deviations, respectively ( $n = 2$ ). Lane 1, the parental control PC9; 2, *vp2vp3mnp2mnp3mnp6lac2m#1*; 3, *vp2vp3mnp2mnp3mnp6lac2m#2*. The bars represent the standard deviation ( $n = 2$ ).

*2mnp3mnp6lac2m#1* and *#2* were almost negligible. These results suggest that *vp2/vp3/mnp2/mnp3/mnp6* and *vp2/vp3/mnp2/mnp3/mnp6/lac2* mutations, but not *vp2/vp3/mnp3/mnp6/lac2*, drastically reduce the lignin-degrading ability of *P. ostreatus* on BWS.

As Figure 5A,B shows the lesser the mutants degraded lignin, the lower the selectivity of lignin degradation was. This phenomenon may be due to elevated polysaccharide-degrading enzyme expression in deficient lignin degradation or structural modification of the remaining lignin that is not indicated by the weight of the acid-insoluble lignin.

### The remaining four *mnp* and *vp* genes were not upregulated in the sextuple-gene mutants on BWS

To examine whether the sextuple-gene mutation affects the transcription level of the remaining four *mnp/vp* genes (*vp1*, *mnp1*, *mnp4*, and *mnp5*), qRT-PCR using real-time PCR was conducted on PC9 and the two sextuple mutants grown on BWS for 13 and 20 days. As shown in Figure 6, transcript accumulation (relative expression level) of *mnp4* was indifferent between the sextuple-gene mutants and the parental control PC9, whereas that of the remaining three, *vp1*, *mnp1*, and *mnp5*, was smaller at 13-day and/or 20-day culture period. Combined with the results in Figure 4C, this result suggests that genes encoding enzymes involved in lignin degradation may not be upregulated in the *vp2/vp3/mnp2/mnp3/mnp6/lac2* mutants on BWS.

### The sextuple-gene mutants also hardly degraded lignin in Japanese Cedar and rice straw

We analysed the lignin-degrading abilities of the sextuple-gene mutants on the different lignocellulosic

substrates/media, toluene/ethanol-extracted Japanese Cedar (softwood *Cryptomeria japonica*), wood sawdust medium (CWS), and the extracted milled rice (grass *Oryza sativa*) straw medium (RS), in which chemical compositions differ from that in beech (hardwood; Katahira et al., 2018; Umezawa et al., 2020). First, each *mnp/vp* transcript was quantified using a digital PCR on 20b grown on BWS-I, CWS, and RS to analyse/compare transcriptional expression patterns/levels. Figure 7A shows that *vp2* and *vp3* transcripts were predominant among *vp/mnp* when grown on CWS, RS, and BWS-I.

Next, PC9 and the two *vp2/vp3/mnp2/mnp3/mnp6/lac2* sextuple-gene mutants were grown on CWS and RS for 30 days, followed by analyses of the decreased amount of Klason lignin. As shown in Figure 7B,C, like the BWS-II case, the ‘Lignin loss’ of *vp2vp3mnp2mnp3mnp6lac2m#1* and *#2* were drastically smaller than that of PC9. These results suggest that the sextuple mutants lose the ability to completely degrade the different natural lignins.

Considering the ‘Composition change’ in Figure S6, it was suggested that the amount of polysaccharide degraded by the sextuple-gene mutants is not reduced compared with that of lignin when grown on CWS, RS, and BWS-II.

## DISCUSSION

In this study, multiple-gene mutants (at maximum sextuple) of *P. ostreatus mnp/vp/lac* were generated using plasmid-based CRISPR/Cas9, and their lignin-degrading abilities were examined/compared. Although the ectopic integration of the transforming plasmid(s) and/or off-target effects cannot be excluded, the results showed that VPs and MnPs (and Lacs) are crucial factors in lignin degradation by *P. ostreatus* on the three lignocellulosic media: BWS, CWS, and RS. Reduced lignin-degrading abilities were observed in the *vp2/vp3/*

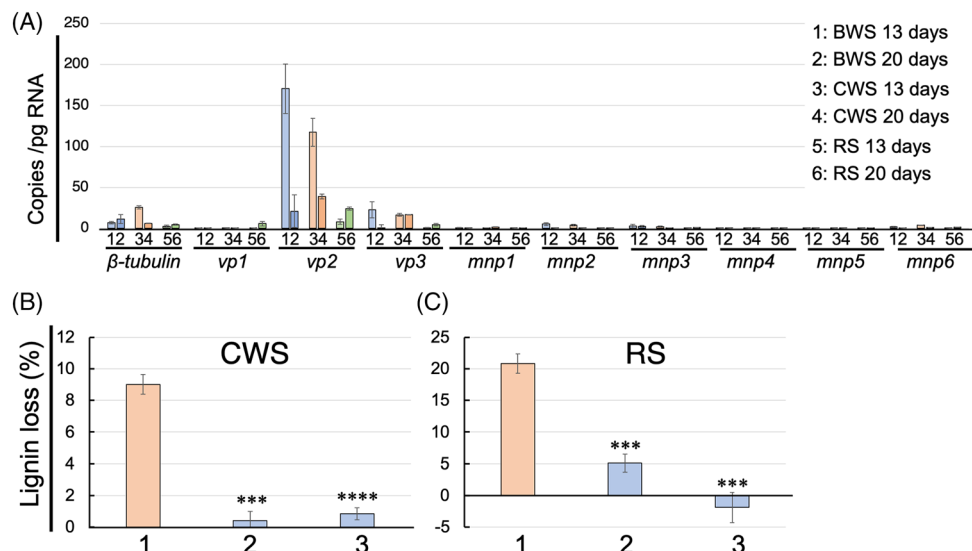


**FIGURE 7** The lignin-degrading abilities of the sextuple-gene mutants on CWS and RS. (A) Transcriptional expression pattern of *mnp/vp* genes in the *Pleurotus ostreatus* 20b strain on BWS-I, CWS, and RS analysed using quantitative reverse transcription-polymerase chain reaction (PCR) with the digital PCR. The bars represent the standard deviation ( $n = 2$ ). (B) The ability of the sextuple-gene mutants to degrade lignin on CWS and RS. The indicated strains (1–3) were grown for 30 days. Strain 1, the parental control PC9; 2, *vp2vp3mnp2mnp3mnp6lac2m#1*; 3, *vp2vp3mnp2mnp3mnp6lac2m#2*. The decreased amount of Klason lignin was compared with that in the No-fungus control plate (onto which *P. ostreatus* was not inoculated). The graphs and bars represent the average and standard deviations, respectively ( $n = 3$ ). A statistical significance test between each mutant and its parental control (Lane 1) was conducted using a two-tailed equal variance *t*-test. \* $p < 0.05$ , \*\* $p < 0.01$ , \*\*\* $p < 0.001$ , \*\*\*\* $p < 0.0001$ , and \*\*\*\*\* $p < 0.00001$ . 'ns' indicates statistical non-significance ( $p > 0.05$ ).

*mnp2/mnp3/mnp6* mutants on BWS, but not in *vp2/vp3/mnp3/mnp6*. Considering that the sum of TPM values of the former five genes (the latter four genes) accounts for 96%–99% (90%–95%) of the nine *mnp/vp* on BWS, high expression/activities of MnPs and VPs may not be required for efficient degradation of natural lignin in lignocellulose by *P. ostreatus* under the cultural conditions used in this work.

Catalytic properties of MnPs, VPs, and LiPs have been extensively studied. For example, MnPs oxidize  $Mn^{2+}$  to  $Mn^{3+}$  (Gold & Glenn, 1988), which attacks lignin model compounds (both phenolic and non-phenolic) directly or via the generation of radicals (Hofrichter, 2002). LiPs directly oxidize non-phenolic aromatic substrates without mediators (Doyle et al., 1998). VPs catalyse both reactions (Ruiz-Dueñas et al., 1999). Multiple copies of LME-encoding genes are predicted in the genomes of all white-rot fungi (Riley et al., 2014). In *P. ostreatus*, a total of nine *mnp* and *vp* genes are predicted in its genome, and expression patterns of *mnp/vp* in the lignocellulose medium (mixture of milled rice straw and poplar) depend on pH and temperature (Fernández-Fueyo, Castanera, et al., 2014). Catalytic properties (kinetic constants for substrates, including  $Mn^{2+}$  and  $H_2O_2$ ) and pH stabilities were different among *P. ostreatus* MnPs/VPs heterologously expressed in *Escherichia coli* (Fernández-Fueyo, Ruiz-Dueñas, et al., 2014). Thus, we hypothesized that *Pleurotus* spp. possibly use different combinations of LMEs to survive different environments/

conditions, allowing a significant number of *Pleurotus* spp. for worldwide distribution throughout hardwood forests under different climates (Vilgalys & Sun, 1994). This could be why they need multiple/redundant copies of LME-encoding genes for survival. Currently, it remains unclear whether there is also high redundancy among LMEs in the other white-rot fungi.

In this study, significantly and greatly higher extracellular cellobiosidase activities were observed in the two sextuple-gene mutants at the 20-day and 30-day periods. This result suggests that cellulose-degrading enzyme-encoding genes may be upregulated in the ligninolytic-deficient mutants so that they can obtain nutrients from polysaccharides in BWS. Considering that many polysaccharide-degrading enzyme-encoding genes, as well as lignin-degrading one, are predicted in the genome of *P. ostreatus* (Riley et al., 2014), future studies will be needed to analyse transcriptional expression in the sextuple-gene mutants to reveal which/what enzyme-encoding genes are upregulated and to elucidate the mechanisms by which they are regulated.

Other peroxidases, including dye-decolorizing peroxidases (EC1.11.1.19) and chloride peroxidases (CPOs; EC1.11.1.10), were also shown to oxidize/cleave  $\beta$ -O-4 in lignin model compounds and/or depolymerize synthetic lignin *in vitro* (Ortiz-Bermudez et al., 2003; Sugano & Yoshida, 2021). Putative four DyP-encoding genes and four CPOs-encoding ones are predicted in the genome of *P. ostreatus*. However,



considering that the ability was almost impaired in the sextuple mutants of *mnp/vp/lac*, these peroxidases are unimportant or required for wood lignin degradation by *P. ostreatus*.

In conclusion, this study provided solid evidence that LMEs (especially VPs and MnPs) are crucial for lignin degradation in plant biomass by *P. ostreatus* for the first time. Considering that the production of only a small amount of VPs/MnPs is sufficient for lignin degradation by *P. ostreatus*, it may be interesting to study and modify the mechanisms of transportation of the degraded lignin fragments into hyphal cells and/or its metabolism/mineralization for enhancing/improving the lignin-degrading ability and utilizing it for biorefineries. However, it remains unclear whether this conclusion applies to lignin degradation by *P. ostreatus* on non-milled substrates, such as wood blocks and wafers, because the expression patterns of *mnp/vp* on these substrates differed significantly from those on the milled substrates (Fernández-Fueyo et al., 2016; Zhang et al., 2019). This should be investigated in the future.

## AUTHOR CONTRIBUTIONS

**Takehito Nakazawa:** Conceptualization (supporting); data curation (lead); formal analysis (lead); funding acquisition (supporting); investigation (equal); methodology (equal); project administration (supporting); supervision (supporting); validation (lead); visualization (lead); writing-original draft (lead). **Iori Yamaguchi:** Formal analysis (lead); investigation (lead); methodology (equal); writing-original draft (supporting). **Yufan Zhang:** Investigation (supporting); methodology (equal). **Chinami Saka:** Data curation (supporting); formal analysis (supporting); investigation (supporting). **Hongli Wu:** Formal analysis (supporting); investigation (supporting); validation (supporting). **Keita Kayama:** Formal analysis (supporting); validation (supporting). **Moriyuki Kawauchi:** Writing-review and editing (supporting). **Masahiro Sakamoto:** Writing-review and editing (supporting). **Yoichi Honda:** Conceptualization (lead); funding acquisition (lead); writing-review and editing (lead).

## ACKNOWLEDGEMENTS

This work was supported in part by the Grants-in-Aid for Scientific Research (KAKENHI) [18H02254, 18KK0178, 19K22332, and 21K18224, 19F19095 to Yoichi Honda; 19H03017 to Takehito Nakazawa] and JSPS Bilateral Program (JPJSBP) [120208402 and 120209920 to Yoichi Honda]. We thank Prof. Antonio Gerardo Pisabarro (Public University of Navarra, Spain) for providing *P. ostreatus* strain PC9, Prof. Yitzhak Hadar (Hebrew University of Jerusalem, Israel) for providing *P. ostreatus* strain 20b, and Prof. Keishi Osakabe (Tokushima University, Japan) for providing plasmid pCcPef3-126.

## CONFLICT OF INTEREST STATEMENT

The authors have no conflicts of interest directly relevant to the content of this article.

## DATA AVAILABILITY STATEMENT

All data supporting the claims of this article are presented and made available in this article and Supporting Information.

## ORCID

Takehito Nakazawa  <https://orcid.org/0000-0002-9654-2124>

Yoichi Honda  <https://orcid.org/0000-0002-7218-7367>

## REFERENCES

- Adinarayana, R. (1995) The potential for white-rot fungi in the treatment of pollutants. *Current Opinion in Biotechnology*, 6, 320–328. Available from: [https://doi.org/10.1016/0958-1669\(95\)80054-9](https://doi.org/10.1016/0958-1669(95)80054-9)
- Arantes, V. & Goodell, B. (2014) Current understanding of brown-rot fungal biodegradation mechanisms: a review. In: Schultz, T.P., Goodell, B. & Nicholas, D.D. (Eds.) *Deterioration and protection of sustainable biomaterials*. Washington: ACS Publications, pp. 3–21. Available from: <https://doi.org/10.1021/bk-2014-1158.ch001>
- Boontawon, T., Nakazawa, T., Horii, M., Tsuzuki, M., Kawauchi, M., Sakamoto, M. et al. (2021) Functional analysis of *Pleurotus ostreatus pcc1* and *clp1* using CRISPR/Cas9. *Fungal Genetics and Biology*, 154, 103599. Available from: <https://doi.org/10.1016/j.fgb.2021.103599>
- Boontawon, T., Nakazawa, T., Inoue, C., Osakabe, K., Kawauchi, M., Sakamoto, M. et al. (2021) Efficient genome editing with CRISPR/Cas9 in *Pleurotus ostreatus*. *AMB Express*, 11, 30. Available from: <https://doi.org/10.1186/s13568-021-01193-w>
- Cragg, S.M., Beckham, G.T., Bruce, N.C., Bugg, T.D.H., Distel, D.L., Dupree, P. et al. (2015) Lignocellulose degradation mechanisms across the tree of life. *Curr Opin in Chemical Biology*, 29, 108–119. Available from: <https://doi.org/10.1016/j.cbpa.2015.10.018>
- del Cerro, C., Erickson, E. & Dong, T. (2021) Intracellular pathways for lignin catabolism in white-rot fungi. *Proceedings of the National Academy of Sciences of the United States of America*, 118, e2017381118. Available from: <https://doi.org/10.1073/pnas.2017381118>
- Doyle, W.A., Blodig, W., Veitch, N.C., Piontek, K. & Smith, A.T. (1998) Two substrate interaction sites in lignin peroxidase revealed by site-directed mutagenesis. *Biochemistry*, 37, 15097–15105. Available from: <https://doi.org/10.1021/bi981633h>
- Eggert, C., Temp, U., Dean, J.F.D. & Eriksson, K.L. (1996) A fungal metabolite mediates degradation of non-phenolic lignin structures and synthetic lignin by laccase. *FEBS Letters*, 391, 144–148. Available from: [https://doi.org/10.1016/0014-5793\(96\)00719-3](https://doi.org/10.1016/0014-5793(96)00719-3)
- Engler, C., Kandzia, R. & Marillonnet, S. (2008) A one pot, one step, precision cloning method with high throughput capability. *PLoS One*, 3, e3647. Available from: <https://doi.org/10.1371/journal.pone.0003647>
- Fernández-Fueyo, E., Castanera, R., Ruiz-Dueñas, F.J., López-Lucendo, M.F., Ramírez, L., Pisabarro, A.G. et al. (2014) Lignolytic peroxidase gene expression by *Pleurotus ostreatus*: differential regulation in lignocellulose medium and effect of temperature and pH. *Fungal Genetics and Biology*, 72, 150–161. Available from: <https://doi.org/10.1016/j.fgb.2014.02.003>
- Fernández-Fueyo, E., Ruiz-Dueñas, F.J., López-Lucendo, M.F., Pérez-Boada, M., Rencoret, J., Gutiérrez, A. et al. (2016) A

- secretomic view of woody and nonwoody lignocellulose degradation by *Pleurotus ostreatus*. *Biotechnology for Biofuels*, 9, 49. Available from: <https://doi.org/10.1186/s13068-016-0462-9>
- Fernández-Fueyo, E., Ruiz-Dueñas, F.J., Martínez, M.J., Romero, A., Hammel, K.E., Medrano, F.J. et al. (2014) Ligninolytic peroxidase genes in the oyster mushroom genome: heterologous expression, molecular structure, catalytic and stability properties, and lignin-degrading ability. *Biotechnology for Biofuels*, 7, 2. Available from: <https://doi.org/10.1186/1754-6834-7-2>
- Floudas, D., Binder, M., Riley, R., Barry, K., Blanchette, R.A. & Henrissat, B. (2012) The Paleozoic origin of enzymatic lignin decomposition reconstructed from 31 fungal genomes. *Science*, 336, 1715–1719. Available from: <https://doi.org/10.1126/science.1221748>
- Gold, M.H. & Glenn, J.K. (1988) Manganese peroxidase from *Phanerochaete chrysosporium*. *Methods in Enzymology*, 161, 258–264. Available from: [https://doi.org/10.1016/0076-6879\(88\)61027-5](https://doi.org/10.1016/0076-6879(88)61027-5)
- Harvey, P.J., Schoemaker, H.E. & Palmer, J.M. (1986) Veratryl alcohol as a mediator and the role of radical cations in lignin biodegradation by *Phanerochaete chrysosporium*. *FEBS Letters*, 195, 242–246. Available from: [https://doi.org/10.1016/0014-5793\(86\)80168-5](https://doi.org/10.1016/0014-5793(86)80168-5)
- Hatakka, A. (1994) Lignin-modifying enzymes from selected white-rot fungi: production and role from in lignin degradation. *FEMS Microbiology Reviews*, 13, 125–135. Available from: <https://doi.org/10.1111/j.1574-6976.1994.tb00039.x>
- Higuchi, T. (2004) Microbial degradation of lignin: role of lignin peroxidases, manganese peroxidase, and laccase. *Proceedings of the Japan Academy, Series B*, 80, 204–214. Available from: <https://doi.org/10.2183/pjab.80.204>
- Hofrichter, M. (2002) Review: lignin conversion by manganese peroxidase (MnP). *Enzyme and Microbial Technology*, 4, 454–466. Available from: [https://doi.org/10.1016/S0141-0229\(01\)00528-2](https://doi.org/10.1016/S0141-0229(01)00528-2)
- Honda, Y., Matsuyama, T., Irie, T., Watanabe, T. & Kuwahara, M. (2000) Carboxin resistance transformation of the homobasidiomycete fungus *Pleurotus ostreatus*. *Current Genetics*, 37, 209–212. Available from: <https://doi.org/10.1007/s002940050521>
- Kamitsuji, H., Honda, Y., Watanabe, T. & Kuwahara, M. (2004) Production and induction of manganese peroxidase isozymes in a white-rot fungus *Pleurotus ostreatus*. *Applied Microbiology and Biotechnology*, 65, 287–294. Available from: <https://doi.org/10.1007/s00253-003-1543-9>
- Katahira, R., Elder, T.J. & Beckman, G.T. (2018) A brief introduction to lignin structure. In: Beckman, G.T. (Ed.) *Lignin valorization: emerging approaches*. London: Royal Society of Chemistry, pp. 1–20. Available from: <https://doi.org/10.1039/9781788010351-00001>
- Keasling, J., Martin, H.G., Lee, T.S., Mukhopadhyay, A., Singer, S.W. & Sundstrom, E. (2021) Microbial production of advanced biofuels. *Nature Reviews. Microbiology*, 19, 701–715. Available from: <https://doi.org/10.1038/s41579-021-00577-w>
- Kersten, P. & Cullen, D. (2014) Copper radical oxidases and related extracellular oxidoreductases of wood-decay agaricomycetes. *Fungal Genetics and Biology*, 72, 124–130. Available from: <https://doi.org/10.1016/j.fgb.2014.05.011>
- Khan, M.I., Shin, J.H. & Kim, J.D. (2018) The promising future of microalgas: current status, challenges, and optimization of a sustainable and renewable industry for biofuels, feed, and other products. *Microbial Cell Factories*, 17, 36. Available from: <https://doi.org/10.1186/s12934-018-0879-x>
- Kirk, T.K. & Farrell, R.L. (1987) Enzymatic ‘combustion’: the microbial degradation of lignin. *Annual Review of Microbiology*, 41, 465–505. Available from: <https://doi.org/10.1146/annurev.mi.41.100187.002341>
- Knop, D., Yarden, O. & Hadar, Y. (2015) The ligninolytic peroxidases in the genus *Pleurotus*: divergence in activities, expression, and potential applications. *Applied Microbiology and Biotechnology*, 99, 1025–1038. Available from: <https://doi.org/10.1007/s00253-014-6256-8>
- Kondo, R., Iimori, T., Imamura, H. & Nishida, T. (1990) Polymerization of DHP and depolymerization of DHP-glucoside by lignin oxidizing enzymes. *Journal of Biotechnology*, 13, 2–3. Available from: [https://doi.org/10.1016/0168-1656\(90\)90103-I](https://doi.org/10.1016/0168-1656(90)90103-I)
- Koshi, D., Ueshima, H., Kawachi, M., Nakazawa, T., Sakamoto, M., Hirata, M. et al. (2022) Marker-free genome editing in the edible mushroom, *Pleurotus ostreatus*, using transient expression of genes required for CRISPR/Cas9 and for selection. *Journal of Wood Science*, 68, 27. Available from: <https://doi.org/10.1186/s10086-022-02033-6>
- Larraya, L.M., Pérez, G., Peñas, M.M., Baars, J.J.P., Mikosch, T.S.P., Pisabarro, A.G. et al. (1999) Molecular karyotype of the white rot fungus *Pleurotus ostreatus*. *Applied and Environmental Microbiology*, 65, 3413–3417. Available from: <https://doi.org/10.1128/aem.65.8.3413-3417.1999>
- Mainka, H., Täger, O., Körner, E., Hilfert, L., Busse, S., Edelmann, F. T. et al. (2015) Lignin – an alternative precursor for sustainable and cost-effective automotive carbon fiber. *Journal of Materials Research and Technology*, 4, 283–296. Available from: <https://doi.org/10.1016/j.jmrt.2015.03.004>
- Marzullo, L., Cannio, R., Giardina, P., Santini, M.T. & Sanna, G. (1995) Veratryl alcohol oxidase from *Pleurotus ostreatus* participates in lignin biodegradation and prevents polymerization of laccase-oxidized substrates. *The Journal of Biological Chemistry*, 270, 3823–3827. Available from: <https://doi.org/10.1074/jbc.270.8.3823>
- Matsunaga, Y., Ando, M., Izumitsu, K., Suzuki, K., Honda, Y. & Irie, T. (2017) A development and an improvement of selectable markers in *Pleurotus ostreatus* transformation. *Journal of Microbiological Methods*, 134, 27–29. Available from: <https://doi.org/10.1016/j.mimet.2017.01.007>
- Miyauchi, S., Navarro, D., Chevret, D. & Berrin, J. (2017) The integrative omics of white-rot fungus *Pycnoporus coccineus* reveals co-regulated CAZymes for orchestrated lignocellulose breakdown. *PLoS One*, 4, e0175528. Available from: <https://doi.org/10.1371/journal.pone.0175528>
- Muraguchi, H., Ito, Y., Kamada, T. & Yanai, S.O. (2003) A linkage map of the basidiomycete *Coprinus cinereus* based on random amplified polymeric DNAs and restriction fragment. *Fungal Genetics and Biology*, 40, 93–102. Available from: [https://doi.org/10.1016/S1087-1845\(03\)00087-2](https://doi.org/10.1016/S1087-1845(03)00087-2)
- Nakazawa, T. & Honda, Y. (2015) Absence of a gene encoding cytosine deaminase in the genome of the agaricomycete *Coprinopsis cinerea* enables simple marker recycling through 5-fluorocytosine counter-selection. *FEMS Microbiology Letters*, 362, fnv123. Available from: <https://doi.org/10.1016/j.funbio.2016.06.011>
- Nakazawa, T., Inoue, C., Morimoto, R., Nguyen, D.X., Bao, D., Kawachi, M. et al. (2023) The lignin-degrading abilities of *Gelatoporia subvermispora gat1* and *pex1* mutants generated via CRISPR/Cas9. *Environmental Microbiology*. Available from: <https://doi.org/10.1111/1462-2920.16372>
- Nakazawa, T., Izuno, A., Horii, M., Kodera, R., Nishimura, H., Hirayama, Y. et al. (2017) Effects of *pex1* disruption on wood lignin biodegradation, fruiting development and the utilization of carbon sources in the white-rot agaricomycete *Pleurotus ostreatus* and non-wood decaying *Coprinopsis cinerea*. *Fungal Genetics and Biology*, 109, 7–15. Available from: <https://doi.org/10.1016/j.fgb.2017.10.002>
- Nakazawa, T., Izuno, A., Kodera, R., Miyazaki, Y., Sakamoto, M., Isagi, Y. et al. (2017) Identification of two mutations that cause defects in the ligninolytic system through an efficient forward genetics in the white rot agaricomycete *Pleurotus ostreatus*. *Environmental Microbiology*, 19, 261–272. Available from: <https://doi.org/10.1111/1462-2920.13595>

- Nakazawa, T., Morimoto, R., Wu, H., Kodera, R., Sakamoto, M. & Honda, Y. (2019) Dominant effects of *gat1* mutations on the ligninolytic activity of the white-rot fungus *Pleurotus ostreatus*. *Fungal Biology*, 123, 209–217. Available from: <https://doi.org/10.1016/j.funbio.2018.12.007>
- Nguyen, D.X., Nakazawa, T., Myo, G., Inoue, C., Kawauchi, M., Sakamoto, M. et al. (2020) A promoter assay using gene targeting in agaricomycetes *Pleurotus ostreatus* and *Coprinopsis cinerea*. *Journal of Microbiological Methods*, 179, 106053. Available from: <https://doi.org/10.1016/j.mimet.2020.106053>
- Niemenmaa, O., Galkin, S. & Hatakka, A. (2008) Ergosterol contents of some wood-rotting basidiomycete fungi grown in liquid and solid culture conditions. *International Biodeterioration & Biodegradation*, 62, 125–134. Available from: <https://doi.org/10.1016/j.ibiod.2007.12.009>
- Nishimura, H., Kamiya, A., Nagata, T., Katahira, M. & Watanabe, T. (2018) Direct evidence for  $\alpha$  ether linkage between lignin and carbohydrates in wood cell walls. *Scientific Reports*, 8, 6538. Available from: <https://doi.org/10.1038/s41598-018-24328-9>
- Ortiz-Bermudez, P., Srebotnik, E. & Hammel, K.E. (2003) Chlorination and cleavage of lignin structures by fungal chloroperoxidases. *Applied and Environmental Microbiology*, 69, 5015–5018. Available from: <https://doi.org/10.1128/AEM.69.8.5015-5018.2003>
- Pezzella, C., Russo, M.E., Marzocchella, A., Salatino, P. & Sannia, G. (2014) Immobilization of a *Pleurotus ostreatus* laccase mixture on perlite and its application to dye decolourisation. *BioMed Research International*, 2014, 308613. Available from: <https://doi.org/10.1155/2014/308613>
- Pfaffl, M.W. (2001) A new mathematical model for relative quantification in real-time RT-PCR. *Nucleic Acids Research*, 29, e45. Available from: <https://doi.org/10.1093/nar/29.9.e45>
- Pickard, M.A., Vandertol, H., Roman, R. & Vazquez-Duhalt, R. (1999) High production of ligninolytic enzymes from white rot fungi in cereal bran liquid medium. *Canadian Journal of Microbiology*, 45, 627–631. Available from: <https://doi.org/10.1139/w98-233>
- Pointing, S.B. (2001) Feasibility of bioremediation by white-rot fungi. *Applied Microbiology and Biotechnology*, 57, 20–32, 33. Available from: <https://doi.org/10.1007/s002530100745>
- Ragauskas, A., Beckham, G., Biddy, M.J., Chandra, R., Chen, F., Davis, M.F. et al. (2014) Lignin valorization: improving lignin processing in the biorefinery. *Science*, 16, 1246843. Available from: <https://doi.org/10.1126/science.1246843>
- Rao, P.S. & Niederpruem, D.J. (1969) Carbohydrate metabolism during morphogenesis of *Coprinus lagopus* (sensu Buller). *Journal of Bacteriology*, 100, 1222–1228.
- Riley, R., Salamov, A.A., Brown, D.W., Nagy, L.G., Floudas, D., Held, B.W. et al. (2014) Extensive sampling of basidiomycete genomes demonstrates inadequacy of the white-rot/brown-rot paradigm for wood decay fungi. *Proceedings of the National Academy of Sciences of the United States of America*, 111, 9923–9928. Available from: <https://doi.org/10.1073/pnas.1400592111>
- Ritter, G.J., Seborg, R.M. & Mitchell, R.L. (1932) Factors affecting quantitative determination of lignin by 72 per cent sulfuric acid method. *Industrial and Engineering Chemistry, Analytical Edition*, 4, 202–204. Available from: <https://doi.org/10.1021/ac50078a017>
- Rosenboom, J., Langer, R. & Traverso, G. (2022) Bioplastics for a circular economy. *Nature Reviews Materials*, 7, 117–137. Available from: <https://doi.org/10.1038/s41578-021-00407-8>
- Ruiz-Dueñas, F.J., Martínez, M.J. & Martínez, A.T. (1999) Molecular characterization of a novel peroxidase isolated from the ligninolytic fungus, *Pleurotus eryngii*. *Molecular Microbiology*, 31, 223–235. Available from: <https://doi.org/10.1046/j.1365-2958.1999.01164.x>
- Salame, T.M., Knop, D., Levinson, D., Mabjeesh, S.J., Yarden, O. & Hadar, Y. (2014) Inactivation of a *Pleurotus ostreatus* versatile peroxidase-encoding gene (*mnp2*) results in reduced lignin degradation. *Environmental Microbiology*, 16, 265–277. Available from: <https://doi.org/10.1111/1462-2920.12279>
- Salame, T.M., Knop, D., Levinson, D., Yarden, O. & Hadar, Y. (2013) Redundancy among manganese peroxidase in *Pleurotus ostreatus*. *Applied and Environmental Microbiology*, 79, 2405–2415. Available from: <https://doi.org/10.1128/AEM.03849-12>
- Salame, T.M., Knop, D., Tal, D., Levinson, D., Yarden, O. & Hadar, Y. (2012) Predominance of a versatile-peroxidase-encoding gene, *mnp4*, as demonstrated by gene replacement via a gene targeting system for *Pleurotus ostreatus*. *Applied and Environmental Microbiology*, 78, 5341–5352. Available from: <https://doi.org/10.1128/AEM.01234-12>
- Salame, T.M., Yarden, O. & Hadar, Y. (2010) *Pleurotus ostreatus* manganese-dependent peroxidase silencing impairs decolourization of Orange II. *Microbial Biotechnology*, 3, 93–106. Available from: <https://doi.org/10.1111/j.1751-7915.2009.00154.x>
- Suetomi, T., Sakamoto, T., Tokunaga, Y., Kameyama, T., Honda, Y., Kamitsuji, H. et al. (2015) Effects of calmodulin on expression of lignin-modifying enzymes in *Pleurotus ostreatus*. *Current Genetics*, 61, 127–140. Available from: <https://doi.org/10.1007/s00294-014-0460-z>
- Sugano, Y. & Yoshida, T. (2021) DyP-type peroxidases: recent advances and perspectives. *International Journal of Molecular Sciences*, 22, 5556. Available from: <https://doi.org/10.3390/ijms22115556>
- Tsukihara, T., Honda, Y., Sakai, R., Watanabe, T. & Watanabe, T. (2006) Exclusive overproduction of recombinant versatile peroxidase MnP2 by genetically modified white rot fungus, *Pleurotus ostreatus*. *Journal of Biotechnology*, 126, 431–439. Available from: <https://doi.org/10.1016/j.jbiotec.2006.05.013>
- Umezawa, T., Tobimatsu, Y., Yamamura, M., Miyamoto, T., Takeda, Y., Koshiba, T. et al. (2020) Lignin metabolic engineering grasses for primary lignin valorization. *Lignin*, 1, 30–41.
- Vilgalys, R. & Sun, B.L. (1994) Ancient and recent patterns of geographic speciation in the oyster mushroom *Pleurotus* revealed by phylogenetic analysis of ribosomal DNA sequences. *Proceedings of the National Academy of Sciences of the United States of America*, 91, 4599–4603. Available from: <https://doi.org/10.1073/pnas.91.10.4599>
- Watanabe, T. & Koshijima, T. (1988) Evidence for an ester linkage between lignin and glucuronic acid in lignin-carbohydrate complex by DDQ-oxidation. *Agricultural and Biological Chemistry*, 52, 2953–2955. Available from: <https://doi.org/10.1271/bbb1961.52.2953>
- Wu, H., Nakazawa, T., Morimoto, R., Shivani Sakamoto, M. & Honda, Y. (2021) Targeted disruption of *hir1* alters the transcriptional expression pattern of putative lignocellulolytic genes in the white-rot fungus *Pleurotus ostreatus*. *Fungal Genetics and Biology*, 147, 103507. Available from: <https://doi.org/10.1016/j.fgb.2020.103507>
- Wu, H., Nakazawa, T., Takenaka, A., Kodera, R., Morimoto, R., Sakamoto, M. et al. (2020) Transcriptional shifts in delignification-defective mutants of the white-rot fungus *Pleurotus ostreatus*. *FEBS Letters*, 594, 3182–3199. Available from: <https://doi.org/10.1002/1873-3468.13890>
- Wu, H., Nakazawa, T., Xu, H., Yang, R., Bao, D., Kawauchi, M. et al. (2021) Comparative transcriptional analyses of *Pleurotus ostreatus* mutants on beech wood and rice straw shed light on substrate-biased gene regulation. *Applied Microbiology and Biotechnology*, 105, 1175–1190. Available from: <https://doi.org/10.1111/1462-2920.13360>
- Xu, H., Nakazawa, T., Zhang, Y., Oh, M., Bao, D., Kawauchi, M. et al. (2022) Introducing multiple-gene mutations in *Pleurotus ostreatus* using a polycistronic tRNA and CRISPR guide RNA strategy. *FEMS Microbiology Letters*, 369, fnac102. Available from: <https://doi.org/10.1093/femsle/fnac102>
- Yamasaki, F., Nakazawa, T., Oh, M., Bao, D., Kawauchi, M., Sakamoto, M. et al. (2022) Gene targeting of dikaryotic *Pleurotus ostreatus* nuclei using the CRISPR/Cas9 system. *FEMS Microbiology Letters*, 369, fnac083. Available from: <https://doi.org/10.1093/femsle/fnac083>

- Zhang, J., Silverstein, K.A.T., Castaño, J.D., Figueroa, M. & Schilling, J.S. (2019) Gene regulation shifts shed light on fungal adaptation in plant biomass decomposers. *mBio*, 10, e02176-19. Available from: <https://doi.org/10.1128/mBio.02176-19>
- Zolan, M.E. & Pukkila, P.J. (1986) Inheritance of DNA methylation in *Coprinus cinereus*. *Molecular and Cellular Biology*, 6, 195–200. Available from: <https://doi.org/10.1128/mcb.6.1.195>

## SUPPORTING INFORMATION

Additional supporting information can be found online in the Supporting Information section at the end of this article.

**How to cite this article:** Nakazawa, T., Yamaguchi, I., Zhang, Y., Saka, C., Wu, H., Kayama, K. et al. (2023) Experimental evidence that lignin-modifying enzymes are essential for degrading plant cell wall lignin by *Pleurotus ostreatus* using CRISPR/Cas9. *Environmental Microbiology*, 25(10), 1909–1924. Available from: <https://doi.org/10.1111/1462-2920.16427>